Engineering Solid Mechanics (2018) 143-154

Contents lists available at GrowingScience

Engineering Solid Mechanics

homepage: www.GrowingScience.com/esm

Instantaneous deflection of self-compacting and lightweight concrete slabs at early-age

Behnam Vakhshouri[a*] and Shami Nejadi[b]

[a]*PhD candidate, Center for Built Infrastructures (CBIR), School of civil and environmental engineering, University of Technology Sydney (UTS), Sydney, Australia*
[b]*A. Professor, Center for Built Infrastructures (CBIR), School of civil and environmental engineering, University of Technology Sydney (UTS), Sydney, Australia*

ARTICLEINFO

Article history:
Received 22 November, 2017
Accepted 18 February 2018
Available online
18 February 2018

Keywords:
Instantaneous deflection
Early-age loading
Slab
Lightweight concrete
Self-compacting concrete
Effective moment of inertia

ABSTRACT

This paper describes laboratory tests on twelve simply-supported one-way slabs including four lightweight concrete slabs in this study and previously conducted experiments on eight self-compacting reinforced concrete slabs subjected to loading at the age of 14 days. All slab were identical by dimensions of 3.8 m long supported on 3.5 m span, 400 mm wide, and 161 mm deep with 4N12 bars at an effective depth of 136 mm providing a reinforcement ratio of 0.008. After seven days moist-curing, the specimens were removed from the formworks and subjected to different values of the uniformly distributed loading including the self-weight of slabs. The mid-span deflection of slabs was recorded immediately after putting the loading blocks on the slabs. Despite close values of the compressive strength of the mixtures, the obtained results validate the effect of the concrete type on the instantaneous deflection of slabs. A wide range of existing models of the effective stiffness of reinforced concrete section were investigated to predict the instantaneous deflection of slabs. Majority of the models are developed for conventional concrete. Comparing the predicted and experimental results of mid-span deflection confirmed that the existing models are inadequate for lightly reinforced specimens such as slabs. New models are proposed and verified to predict the effective moment of inertia in the slabs with and without fiber reinforcing concretes.

1. Introduction

Determination of the deflection in structure is important from serviceability criteria. Despite importance of the flexural deflection in serviceability design of reinforced concrete structures, simplified methods to predict the deflection in design codes are not compatible with the experimental deflection values under the service loads (Newhook, 2001). In sensitive elements such as slabs with lightly-reinforced concrete section, the long-term deflection is the governing factor in design for serviceability aspects and required performance (Gilbert, 2007).

* Corresponding author.
E-mail addresses: behnam.vakhshouri@student.uts.edu.au (B. Vakhshouri)

doi: 10.5267/j.esm.2018.2.001

The flexural deflection of reinforced concrete members is computed using the effective flexural stiffness to account for non-linear behavior of the section after the concrete has cracked (Bischoff & Darabi, 2012). Differences between the various methods used to estimate the flexural deflection depend on various factors. The main effective factors are the shape of the curvature diagram along the span, which in turn, is affected by the service load type and level, boundary conditions, ratio of the cracking moment and moment of inertia to those for service load and the ultimate capacity of section and tension stiffening (Bischoff & Gross, 2010).

Design codes generally predict the time-dependent deflection by multiplying an empirical amplification factor by an instantaneous deflection at the age of 28 days. This multiplier might be affected by material properties, loading value and section properties (Vollum, 2003). However, the early-age loading of slabs might be inevitable in construction industry. Effect of the early-age loading on deflection of concrete slabs is not completely understood in the literature; however, it is inevitable effective parameter and complicates the prediction of the instantaneous and time-dependent deflection of reinforced concrete section.

Park et al. (2010) investigated the effective stiffness in conventional concrete slabs subjected to early-age loading and found that ACI 209-08 and ACI- 318-08 overestimate the elastic modulus and underestimate the long-term deflection at early-age loading. Park et al. (2012) investigated the effect of curing condition and low-temperature on the early-age loaded slab specimens and confirmed their previous experiment results (Park et al., 2010). Lee et al. (2007) conducted experimental investigation on slabs subjected to early loading at the ages of 3, 7, and 28 days and found that the early-age loading has significant effect on the instantaneous and long-term deflections. They also showed that overestimation of effective stiffness of reinforced concrete section by provisions of the ACI 318-08 results in the underestimated immediate and long-term deflections of the slabs subjected to the early-age loading.

This study investigates the instantaneous deflection of twelve identical concrete slabs under different magnitudes of service loads. The described research program investigates the influence of the loading level and the effective stiffness on the instantaneous deflection at the age of 14 days ($\Delta_{inst-14}$) of one-way slab specimens manufactured with Lightweight Concrete (LWC) and Self-Compacting Concrete (SCC). The main objectives of this study are:

- Comparing the experimentally recorded values of $\Delta_{inst-14}$ in LWC and SCC slabs
- Comparing the development rate of the modulus of elasticity and compressive strength in LWC and SCC mixtures
- Comparing the recorded deflections with the predictions of existing equations of effective moment of inertia (I_e) in codes of practice and empirical equations
- Investigating the effect of loading level, ratio of the applied service moment (M_a) to cracking moment (M_{cr}) and ultimate bending capacity of section (M_u) on Δinst-14
- Investigating the effect of fiber type and content in SCC slabs deflection
- Modifying the existing equations of effective moment of inertia (I_e) to propose new models for LWC and SCC slabs with and without fiber reinforcing

2. Experimental program

Twelve concrete slabs internally reinforced with steel and different types of fiber were constructed and tested to record the instantaneous deflection at the early-age of 14 days. Aslani (2014) conducted series of tests on eight specimens of SCC slabs with 4 pairs of mixture design in the concrete laboratory of University of Technology Sydney (UTS). The authors conducted the second series of tests on four LWC slab specimens with one mixture design. All specimens were similarly simply supported having length 3500 mm (138 in), depth 161 mm (6.3 in) and width 400 mm (15.7 in). The side and bottom cover of concrete from bar centroid were 40 mm (1.6 in) and 25 mm (1 in), respectively.

Each slab was singly reinforced with four symmetrically positioned deformed N steel bars of 12 mm diameter and 3800 mm (150 in) length (including anchorage length). The height and width of the specimen were chosen to allow proper placement of the longitudinal reinforcement and to be able to accommodate the test parameters.

3. Curing and loading of slabs

Each slab was moist cured for 14 days and then the predetermined load level was applied on the slab. To provide the required loading, rectangular concrete blocks of predetermined size and weights were cast and weighed before the commencement of the test. Slab specimens were uniformly loaded by the concrete blocks using wooden timbers as loading pads. The deflection at mid-span of the slab specimen was recorded by Linear Variable Differential Transformer (LVDT). Fig. 1 shows the arrangement of concrete blocks on top of each specimen to achieve the required load level and the LVDT positioning under the slabs.

Lightweight concrete

Self-compacting concrete

Fig. 1. Loading blocks arrangement and LVDT positioning for flexural test of slabs

4. Materials and admixtures

Two different types of concrete; LWC, and SCC have been used to investigate the instantaneous deflection of one-way slabs. Table (1) explains the mixture proportions and density of LWC and SCC mixtures. Type, volume and aspect ratio of the fibers of the SCC mixture are illustrated in Table 1 and Table 2 also.

Table 1. Mixture design of slab specimens

Constituents	N-SCC	D-SCC	S-SCC	DS-SCC	LWC
Cement, kg/m^3 (lb/ft^3)	160 (10)	160 (10)	160 (10)	160 (10)	250 (15.6)
Fly Ash (kg/m^3)	130 (8)	130 (8)	130 (8)	130 (8)	
GGBFS (kg/m^3)	110 (7)	110 (7)	110(7)	110(7)	
Cementitious content (kg/m^3)	400(25)	400(25)	400 (25)	400 (25)	
water	208 (13)	208 (13)	208 (13)	208 (13)	150 (9)
Water Cementitious ratio	0.52	0.52	0.52	0.52	0.6
Aggregate ,kg/m^3 (lb/ft^3)					
Coarse sand	660(41)	660 (41)	660 (41)	660 (41)	620 (39)
fine sand	221(14)	221(14)	221 (14)	221 (14)	
Coarse aggregate	820 (51)	820 (51)	820 (51)	820 (51)	800 (50)
Light Aggregate (BST)					300 (19)
Admixtures ,lit/m^3 (lit/f^3)					
Super plasticizer	4 (0.11)	4.86 (0.14)	4.73 (0.13)	4.5 (0.13)	
Viscosity modifying agent	1.3 (0.04)	1.3 (0.04)	1.3 (0.04)	1.3 (0.04)	
High range water reducing agent	1.6 (0.05)	1.6 (0.05)	1.6 (0.05)	1.6(0.05)	
Fibre content, kg/m^3 (lb/ft^3)					
Steel	-	30 (1.9)	-	15 (0.9)	
Polypropylene	-	-	5	3	
Density, **kg/m^3 (lb/ft^3)**	2340 (146)	2274 (142)	2330 (145)	2385 (149)	2000 (125)

Table 2. The physical and mechanical properties of fibers

Type	Trade name	Density (kg/m^3) (lb/ft^3)	Length Mm (*in*)	Diameter mm(in)	Aspect Ratio (*l*/*d*)	Tensile strength MPa (ksi)	Elasticity modulus GPa(ksi)
Steel	Dramix RC-80/60-BN	7850 (490)	60 (2.4)	0.75 (0.03)	80	1050 (152)	200 (29000)
Polypropylene	Synmix 65	905 (56)	65 (2.6)	0.85(0.33)	76.5	250 (36)	3 (435)

5. Early-age properties of SCC and LWC mixtures

The existing models and empirical relationships to predict the early-age characteristics of SCC and LWC are very rare in the literature. Therefore, precise values of the compressive strength and modulus of elasticity of the mixtures were measured by the companion test specimens in laboratory conditions. Fig. 2 compares the experimental values and development rate of the compressive strength and modulus of elasticity of the mixtures at the ages of 14 and 28 days.

According to Fig. 2, the average increasing ratio of the modulus of elasticity in SCC and LWC are 1.17 and 1.10, respectively. The development ratio of the compressive strength in SCC and LWC are 1.15 and 1.10, respectively.

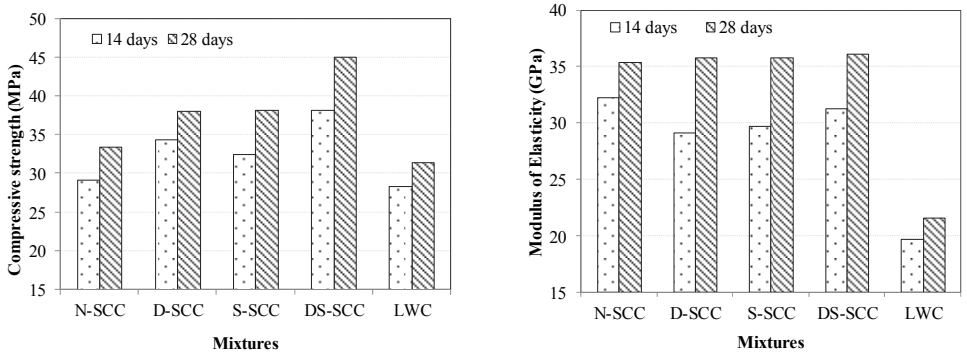

Fig. 2. Compressive strength and modulus of elasticity of mixtures at 14 and 28 days

6. Difference between elastic and instantaneous deflection

Elastic deflection of reinforced concrete structures in some codes of practice is considered as the instantaneous or short-term deflection of slabs. This section compares the experimental instantaneous values with the calculated elastic deflection of the investigated slabs. The instantaneous deflection was recorded by LVDT installed at mid-span, immediately after early-age loading of slabs. Table 3 shows the calculated elastic deflection (Δ_e) based on the modulus of elasticity at the ages of 14 and 28 days. The recorded instantaneous deflection at the age of 14 days ($\Delta_{ins\text{-}14}$) of each slab under different values of the uniformly distributed load (W_a) is presented in the table also. Ultimate capacity of section (M_u), applied service moment due to loading (M_a) and ratio of M_a/M_u are also given in Table (3).

Considering the instantaneous deflection as elastic deflection is a common source of error in design of the concrete structures. Fig. 3 shows the ratio of experimental instantaneous deflection to the calculated elastic deflection at the ages of 14 ($\Delta_{ins\text{-}14}$ / $\Delta_{e\text{-}14}$) and 28 days ($\Delta_{ins\text{-}14}$ / $\Delta_{e\text{-}28}$) of concrete

slabs. According to Fig. 5, the majority of these defections ratio in the slabs are in the range of 1.5 to 2.5.

Table 3 Loading levels and recorded instantaneous and predicted elastic deflection

Slab	W_a (KN/m)	M_u (kN.m)		M_a (kN.m)	M_a / M_u (%)		Δ_e (mm)		Δ_{ins} (mm)
		14 day	28 day		14 day	28 day	14 day	28 day	
N-SCC-a	7.31	27.47	27.78	11.189	40.73	40.27	3.18	2.9	12.1
N-SCC-b	5.41	27.47	27.78	8.28	30.14	29.8	2.36	2.15	5.89
D-SCC-a	7.26	27.84	28.05	11.12	39.94	39.65	3.5	2.85	7.65
D-SCC-b	5.36	27.84	28.05	8.21	29.48	29.27	2.58	2.11	7.59
S-SCC-a	7.3	27.73	28.05	11.18	40.32	39.85	3.45	2.87	6.41
S-SCC-b	5.4	27.73	28.05	8.27	29.83	29.48	2.55	2.12	2.91
DS-SCC-a	7.33	28.05	28.34	11.23	40.03	39.63	3.29	2.85	8.98
DS-SCC-b	5.43	28.05	28.34	8.32	29.66	29.36	2.44	2.11	5.14
LWC-1	7	27.4	27.65	10.72	39.13	38.78	4.99	4.57	11.96
LWC-2	7	27.4	27.65	10.72	39.13	38.78	4.99	4.57	11.4
LWC-3	5.29	27.4	27.65	8.095	29.55	29.28	3.77	3.45	6.3
LWC-4	5.29	27.4	27.65	8.095	29.55	29.28	3.77	3.45	5.98

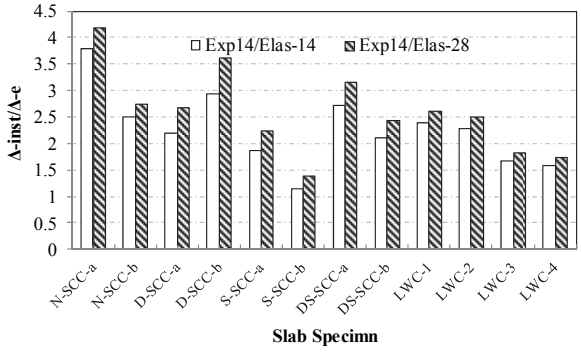

Fig. 3. Ratio of recorded instantaneous deflation to elastic deflection at ages 14 and 28 days

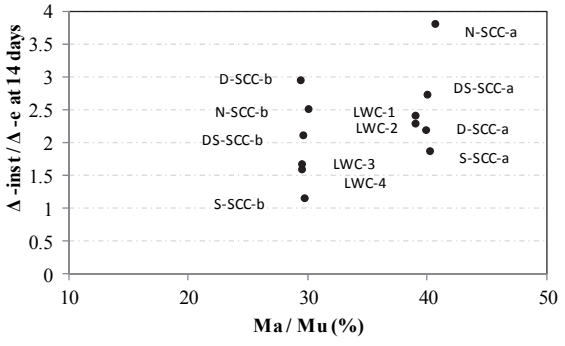

Fig. 4. Instantaneous / elastic deflection ratio at 14 days under different moment ratios

7. Loading effect

Among the effective parameters on the instantaneous deflection of lightly-reinforced concrete structures, the loading rate and Ma/Mu ratio play a major role. Fig. 4 compares the effect of M_a/ M_u ratio on the ratio of $\Delta_{ins\text{-}14}$ / $\Delta_{e\text{-}14}$ in the slabs. The SCC and LWC slabs were loaded by about 30% and 40% of their ultimate moment capacity. Except D-SCC (a, b), the 10% load increment in the slabs resulted in 50 % to 70% increasing of the $\Delta_{ins\text{-}14}$ / $\Delta_{e\text{-}14}$ ratio. Considering the uncertainties in slab design and the unexpected loads during the construction, this amount of loading effect is a crucial parameter in the ultimate design of slabs.

The cracking moment (M_{cr}) causes the first cracking under the flexural loading in the reinforced concrete section. Along with the magnitude of the applied moment, effect of the cracking moment (M_{cr}) is considerable in deflection calculations of the slabs. Since M_{cr} and M_u are dependent characteristics of the slab section, they may change Δ_{ins} / Δ_e ratio in a similar manner. The ratio of M_a/M_u is limited to 30% and 40% in LWC and SCC slabs; in the other words, M_a is related to M_u in this experiment. According to Figure (5) the ratio of $(\Delta_{ins}/\ \Delta_e)_{14}$ varies in different ratios of M_{cr}/ M_u and M_a/ M_u, similarly. However, the ratio of M_{cr}/ M_u is more effective on the instantaneous deflection calculations, particularly in the low-strength concrete specimens.

In all slabs the applied Ma is lower than the M_{cr} and the section is expected to behave in the elastic range. However, due to the creep and shrinkage cracking, the instantaneous deflection is higher than the expected elastic deflection. As presented in Fig. 6 the instantaneous deflection in one-way slabs increases slightly by decreasing the ratio of M_{cr}/M_a; while, it develops by increasing the ratio of M_{cr}/M_u and M_a/M_u.

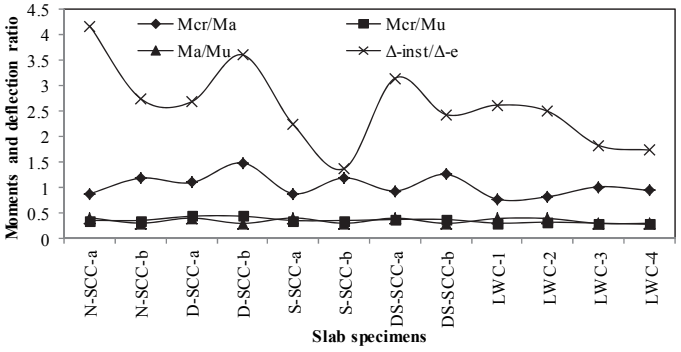

Fig. 5. Effect of moment ratios on Δins / Δe at 14 days

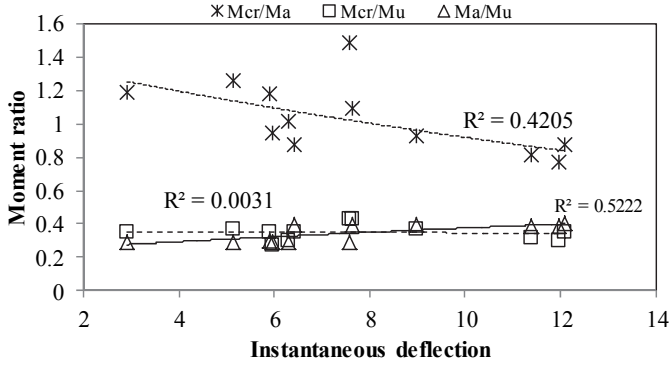

Fig. 6. Effect of moment ratios on instantaneous deflection of slabs at 14 days

8. Effective moment of Inertia

This study investigates the identical slab specimens manufactured with the most frequently used types of normal strength concrete. All slabs have the same support condition, span length, section dimension and bar arrangement. Since the slab geometry, structural and the environmental conditions are the same for all slabs, the bending stiffness can be a critical variable to study the changes in the deflection behavior of slabs in this study.

Continuity of the sections along the span; i.e. variable cross-sections and hence, the variable moment of inertia depending on the degree of cracking along the beam strongly affect the instantaneous deflection. When an RC element cracks, its stiffness does not suddenly change to that of a section where the tension concrete can be fully disregarded (Gilbert, 2007). In fact, the sections where the cracks are localized are separated by regions where the concrete in tension is uncracked with an increase of the stiffness. Behavior at the cracked section used to compute the cracked transformed moment of inertia (I_{cr}) is assumed to be linear elastic. The nonlinearity of the member stiffness is taken into account with an effective moment of inertia (I_e) that models the transition from a gross (uncracked) moment of inertia (I_g) to I_{cr}. Fig. 7 shows cracked and uncracked sections of a simply supported one-way slab under sustained service loading.

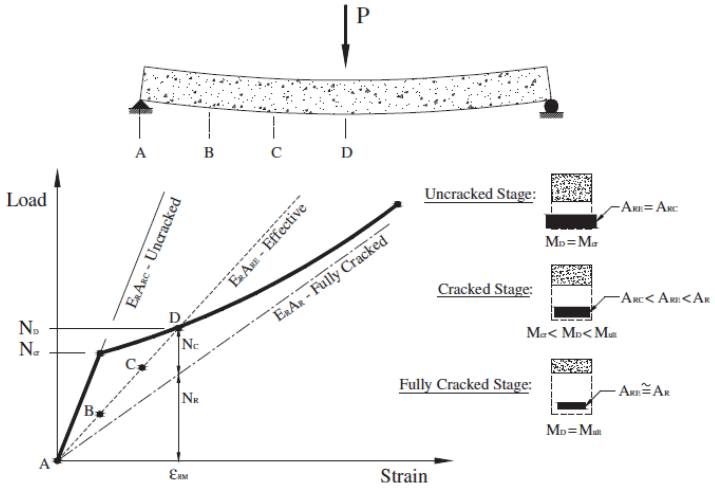

Fig. 7. Deformation Response of Idealized reinforcement at critical section

Branson (1963) and Vakhshouri and Nejadi (2014) introduced the concept of the effective moment of inertia to predict the curvature and deflections directly from the elasticity theory. The concept was verified by different researchers mainly by implementing the idea of tension stiffening to apply for various types of structures, loading rates, fiber reinforced and FRP sheets, and bars included concrete members. Eqs. (1-16) present some verified models of Ie in the literature.

Reference	Equation	Equation
Vakhshouri and Nejadi (2014)	$I_e = (M_{cr}/M_a)^2 I_g + \left(1 - (M_{cr}/M_a)^2\right) I_{cr} \le I_g$ $I_e = (M_{cr}/M_a)^3 I_g + \left(1 - (M_{cr}/M_a)^3\right) I_{cr} \le I_g$ $I_e = (M_{cr}/M_a)^4 I_g + \left(1 - (M_{cr}/M_a)^4\right) I_{cr} \le I_g$	Eq. (1) Eq. (2) Eq. (3)
(Alshaikh and Al-Zaid, 1993)	$I_e = I_{cr} + (I_g - I_{cr})(M_{cr}/M_a)^{3-0.8\rho} \le I_g$	Eq. (4)
ACI-318-08 (2002) ACI-435-68 (1968) AS-3600-09 (2009)	$I_e = (M_{cr}/M_a)^3 I_g + \left(1 - (M_{cr}/M_a)^3\right) I_{cr} \le I_g$	Eq. (5)
ACI 440 (2006)	$I_e = \left(\frac{M_{cr}}{M_a}\right)^3 \beta_d I_g + \left[1 - \left(\frac{M_{cr}}{M_a}\right)^3\right] I_{cr} \le I_g$ $\beta_d = \alpha_b(\frac{E_f}{E_s} + 1),\ \ \beta_d = 0.2\frac{\rho}{\rho_b} < 1$	Eq. (6)
Bischoff and Paixao (2004) Eurocode 2, (1994)	$I_{ef} = \frac{I_{cr}}{1-\eta(M_{cr}/M_a)^2} \le I_g$ $\eta = 1 - Icr/ Ig$	Eq. (7)
Bischoff (2004, 2007) Bischoff and Scanlon (2007)	$I_e = \frac{I_{cr}}{1-\eta\beta(M_{cr}/M_a)} \le I_g$ no tension stiffening $0 \le \beta \le 1$ full tension stiffening	Eq. (8)
Bischoff and Gross (2011)	$I'_e = \frac{I_{cr}}{1-\eta\gamma\beta(M_{cr}/M_a)} \le I_g$ γ=1.72 – 0.72Mcr /Ma , $\beta = M_{cr}/M_a$	Eq. (9)
Faza and GangaRao (1992)	$I_m = \frac{23 I_{cr} I_e}{8 I_{cr} + 15 I_e}$	Eq. (10)
Benmokrane & Masmoudi (1996)	$I_e = \left(\frac{M_{cr}}{M_a}\right)^3 \frac{I_g}{7} + 0.84\left[1 - \left(\frac{M_{cr}}{M_a}\right)^3\right] I_{cr} \le I_g$	Eq. (11)
Yost et al. (2003) ACI-440 (2006)	$I_e = \left(\frac{M_{cr}}{M_a}\right)^3 \beta_d I_g + \left[1 - \left(\frac{M_{cr}}{M_a}\right)^3\right] I_{cr} \le I_g$ $\beta_d = 0.2\frac{\rho}{\rho_b} < 1$	Eq. (12)
Rafi et al. (2008)	$I_e = \left(\frac{M_{cr}}{M_a}\right)^3 \beta_d I_g + \left[1 - \left(\frac{M_{cr}}{M_a}\right)^3\right] \frac{I_{cr}}{\gamma} \le I_g$ $\gamma = (\frac{0.0017\rho}{\rho_b} + 0.8541)(\frac{E_f}{2E_s} + 1)$	Eq. (13)
Alsayed et al. (2000)	$I_e = I_{cr}$ for $\frac{M_{cr}}{M_a} > 3$ $I_e = \left[1.4 - \frac{2}{15}\left(\frac{M_{cr}}{M_a}\right)\right] I_{cr} \le I_g$ for $1 < \frac{M_{cr}}{M_a} < 3$	Eq. (14) Eq. (15)
ISIS Canada (2001)	$I_e = \frac{I_g I_{cr}}{I_{cr} + [1 - 0.5(\frac{M_{cr}}{M_a})^2](I_g - I_{cr})} \le I_g$	Eq. (16)

The equations for the effective moment of inertia have been used to predict and evaluate the instantaneous deflection of the slabs. Fig. 8 compares the ratio of the experimental instantaneous deflections to the predicted values using Eqs. (1-16).

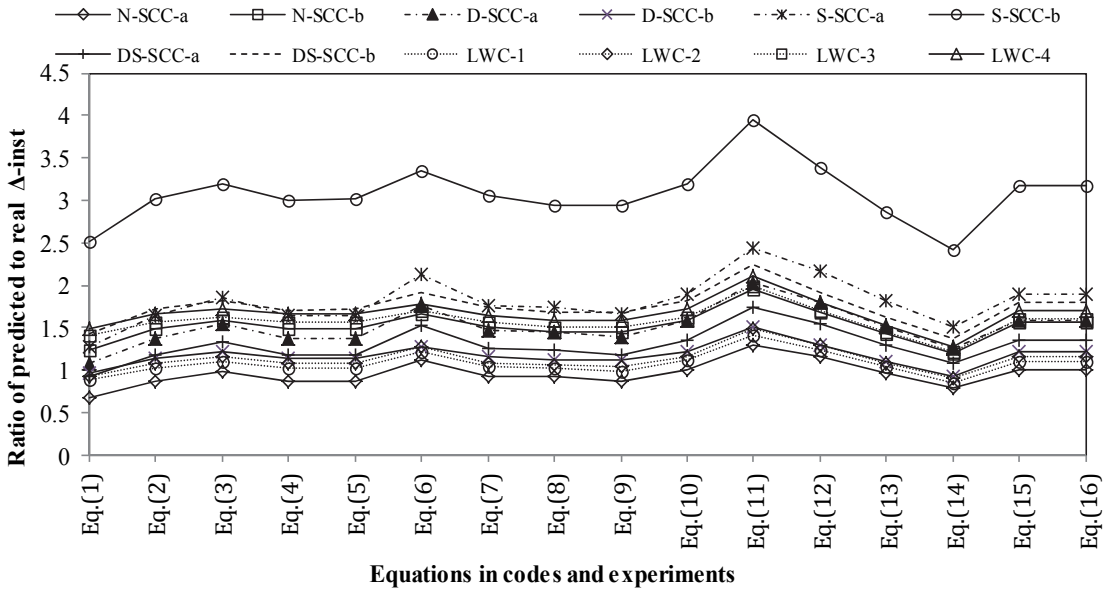

Fig. 8. Comparison of the recorded and predicted instantaneous deflection of slabs

Surprisingly, there are big differences between the predicted and recorded deflections in a majority of the slabs. However each equation gives close predictions for SCC and LWC slabs, and the concrete type has no clear impact on predictions of each equation. The range of the recorded to predicted deflection ratio in most cases are between 0.5 to 1.5, however Eqs. (11-14) give the highest and lowest estimation of the instantaneous deflection in the slabs, respectively. The predictions by Eq. (1), Eq. (5), Eq. (7) and Eq. (14) are the most compatible values with the recorded experimental deflection of slabs with different types of concrete.

The S-SCC-b slab poses the highest estimation of the instantaneous deflection by all equations. Among all slabs, the predicted values in LWC slabs are more reasonable than SCC slabs, and the predictions for fiber reinforced self-compacting concrete are about 30 to 80% higher than the experimental values.

9. Proposed analytical models

The existing models of the effective moment of inertia vary in precision in the estimation and complexity. However, regarding the SCC and FRSCC members, no evidence of such models is found.

Comparison of the existing models and the experimental data shows that the models in Eq. (11) and Eq. (12) give conservative $\Delta_{ins\text{-}14}$ predictions in all slabs. In this study, the required certain intrinsic and/or extrinsic variables (i.e., properties of concrete, support conditions, loading type and loading age) in Ie prediction is properly covered by the presented equations. Besides, the Eq. (1), Eq. (5), Eq. (7) and Eq. (14) give the most compatible prediction of the experimental data. Therefore, the models in Eqs. (1-14) are utilizing as the basis of the proposed model in this study. To attain a better estimation of the instantaneous deflection in the proposed model, the time-dependent elasticity, fiber volume fraction in the mixture, ultimate and cracking moment capacity, and the applied service moment have been included in the equation.

Fiber type, fiber volume fraction and the aspect ratio of the fiber are the main effective parameters in comparison of the fiber reinforced sections, especially in the tensile and flexural behavior. Regarding the negligible difference in the aspect ratio of the applied fibers in the SCC slabs, the effect of type and volume fraction of the fiber on the instantaneous deflection is investigated. In addition, according to the considerable effect of the time-dependent M_u on the moment ratios and deflection in Figs. (6-8), the M_{cr}/M_u ratio is also included in the proposed model. To include the effect of early-age loading, the ratio of modulus of elasticity of concrete at loading age to that of the age of 28 days is applied in the proposed equation.

Eqs. (1-14) are basically developed for beams. Eq. (14) predicts Ie in two distinct ranges of $1<M_{cr}/M_a < 3$ and $M_{cr}/M_a >3$. In addition, and there is no limit for M_{cr}/M_a in the Eq. (1). The ratios of Mcr/Ma and Mcr/Mu for slabs in this study are between 0.63 to 1.72 and 0.29 to 0.47, respectively. Accordingly, the proposed model in this study is recommended to apply for $M_{cr}/M_a < 3$.

Excluding the steel bars from the reinforced section calculations causes about 15% underestimation of Ig in the slabs of this study. Therefore, the transformed section method is utilized to include the reinforcement effect in calculation of the precise Ig of the slabs. Eq. (17) is proposed to predict Ie in SCC slabs with and without fiber reinforcing. The applied coefficients and the limitations are illustrated in Table 4.

$$I_{ef} = \alpha \times I_{cr}\left(M_{cr}/M_a\right)^{(1-0.1V_f)} + \left[(1-\beta) + \frac{M_{cr}^2}{(M_a \times M_u)^{(2+\beta)}}\right] I_g \,, \tag{17}$$

where; ρ is the ratio of the tensile reinforcement in the section, $E_{c\text{-}14}$ and $E_{c\text{-}28}$ (MPa, ksi)) are the modulus of elasticity of SCC at 14 and 28 days respectively, M_{cr}, M_a, M_u (KN.m, lbf.ft)) are cracking moment, service moment and the ultimate capacity of the section respectively. Other coefficients are presented in Table 4.

Table 4. Coefficients and limitations of proposed equation for I_e estimation

I_{ef} , ρ, M_a	Coefficient of fiber type (α)		Ratio of elasticity β	Fiber content V_f
$I_{ef} \le 0.6I_g$ $\rho \ge 0.005$ $M_{cr}/M_a < 3$	α=0.9 α=1.0 α=1.15 α=1.95	for DS-SCC for SCC for D-SCC for S-SCC	β=$E_{c\text{-}14}$/ $E_{c\text{-}28}$ $E_{c\text{-}14}$ and $E_{c\text{-}28}$ Modulus of elasticity of concrete at 14 and 28 days	Fiber volume fraction in the mixture (Kg/m^3) presented in Table 1

Fig. 9 compares the recorded instantaneous deflection of SCC slabs with the prediction of the proposed equation. Obviously, there is a good agreement between the predicted and experimental instantaneous deflection of all SCC slabs.

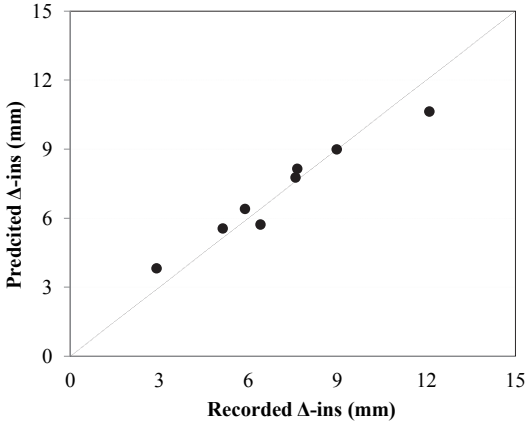

Fig. 9. Comparison of the recorded and predicted deflection of SCC slabs

The LWC slabs in this study were not reinforced with fibers. Therefore, apart from the proposed Eq. (17) for SCC slabs, Eq. (18) is proposed to predict the effective moment of inertia in LWC slabs. The applied coefficients and limitations are described in Table 5.

$$I_{ef} = I_{cr} \times \left(\frac{M_{cr}}{M_a}\right)^2 + \left[(1-\beta) + \frac{(M_{cr})^{1.7}}{(M_a \times M_u)}\right] \times I_g \quad (18)$$

Table 5. Coefficients and limitations of proposed model for Ie in LWC slabs

Coefficient	β	ρ	M_{cr}/M_a	I_{ef}
Limit	$E_{c\text{-}14}/E_{c\text{-}28}$	≥ 0.005	≤ 3	≤ $0.6I_g$

This type of LWC is widely used in Australia; hence, the maximum I_{ef} is recommended to agree with the limitations of AS-3600-09 (2009).

The limitation in the Australia and American standards (AS-3600-09 2009) for the ratio of M_{cr}/M_a is recommended to be applied in the proposed I_e in this study.

The agreement between the experimental values of deflection in LWC and the predicted values by using Eq. (18) is shown in Fig. 10.

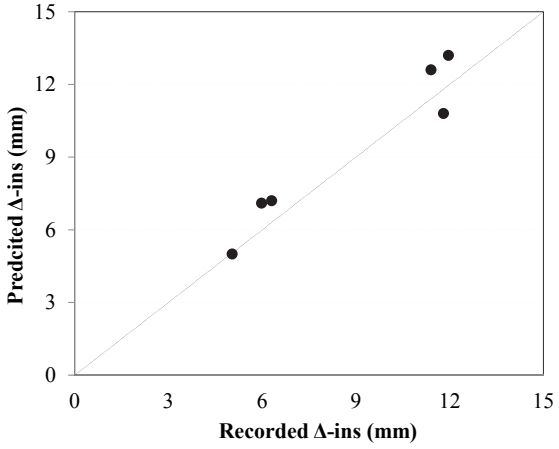

Fig. 10. Comparison of the recorded and predicted deflection of LWC slabs

10. Conclusion

The instantaneous deflection of LWC and SCS slabs was investigated under distinct loading levels in this study. The following conclusions can be drawn from the study:

In the existing models of the effective moment of inertia in the literature there is almost linear relationship between the load value and the instantaneous deflection of slabs. The results of this study contradict this relationship, especially in the low-strength concrete slabs;

The instantaneous deflection due to 10% of load increment increased about 100%, and 105% in the LWC and SCC slabs;

The instantaneous deflection of fiber reinforced SCC slabs shows less variation with changes of the loading level;

Considering the elastic deflection equal to instantaneous deflection even for $M_a < M_{cr}$ in slabs is completely wrong and causes unsafe design of reinforced concrete slabs;

For the early-age loading, the calculations based on the mechanical properties at the age of 28 days may result in wrong predictions of the instantaneous deflection of slabs;

The ratio of service moment to the ultimate moment capacity of slabs strongly affects the instantaneous deflection;

A new model is proposed and verified to predict the effective moment of inertia in SCC slabs; and

A new model of the effective moment of inertia is proposed and verified for the lightweight concrete slabs.

References

ACI-318-02. Building code requirements for structural concrete (ACI 318-08) and commentary. 2002. American Concrete Institute, International Organization for Standardization.

ACI-435, Deflections of reinforced concrete flexural member. American Concrete Institute (ACI), Concrete International, 1968.

ACI-440-06, Guide for the design and construction of concrete reinforced with FRP bars. American Concrete Institute (ACI) Committee 440, ACI 440.1R-06, ACI, Farmington Hills, MI, 44, 2006.

Alsayed, S. H., Al-Salloum, Y. A., & Almusallam, T. H. (2000). Performance of glass fiber reinforced plastic bars as a reinforcing material for concrete structures. *Composites Part B: Engineering, 31*(6-7), 555-567.

Alshaikh, A. H., & Al-Zaid, R. (1993). Effect of reinforcement ratio on the effective moment of inertia of reinforced concrete beams. *Structural Journal, 90*(2), 144-149.

AS-3600-09, Concrete structures. Standards Australia, 2009.

Aslani, F. (2014). Experimental and numerical study of time-dependent behaviour of reinforced self-compacting concrete slabs (Doctoral dissertation).

Benmokrane, B., & Masmoudi, R. (1996). Flexural response of concrete beams reinforced with FRP reinforcing bars. *Structural Journal, 93*(1), 46-55.

Bischoff, P. H. (2007). Deflection calculation of FRP reinforced concrete beams based on modifications to the existing Branson equation. *Journal of Composites for Construction, 11*(1), 4-14.

Bischoff, P. H., & Paixao, R. (2004). Tension stiffening and cracking of concrete reinforced with glass fiber reinforced polymer (GFRP) bars. *Canadian Journal of Civil Engineering, 31*(4), 579-588.

Bischoff, P. H., & Darabi, M. (2012). Unified approach for computing deflection of steel and FRP reinforced concrete. *Special Publication, 284*, 1-20.

Bischoff, P. H., & Gross, S. P. (2010). Equivalent moment of inertia based on integration of curvature. *Journal of Composites for Construction, 15*(3), 263-273.

Darwin, D., Scanlon, A., Gergely, P., Bishara, A. G., Boggs, H. L., Brander, M. E., ... & Liu, T. C. (1986). Cracking of concrete members in direct tension. *Journal of American Concrete Institute*, *83*(1), 3-13.

du Béton, C.E.-I., CEB-FIP model code (MC-90). (1993). Thomas Telford Ltd, London.

Faza, S. S., & GangaRao, H. V. S. (1992). Pre-and post-cracking deflection behaviour of concrete beams reinforced with fibre-reinforced plastic rebars. In Proceedings of the First International Conference on Advance Composite Materials in Bridges and Structures (ACMBS-I), *Canadian Society of Civil Engineers, Sherbrooke*, Cananda (pp. 129-137).

Fikry, A. M., & Thomas, C. (1998). Development of a model for the effective moment of inertia of one-way reinforced concrete elements. *Structural Journal, 95*(4), 445-455.

Gilbert, R. I. (2008). Closure to "Tension Stiffening in Lightly Reinforced Concrete Slabs" by R. Ian Gilbert. *Journal of Structural Engineering, 134*(7), 1264-1265.

Hall, T., & Ghali, A. (2000). Long-term deflection prediction of concrete members reinforced with glass fibre reinforced polymer bars. *Canadian Journal of Civil Engineering, 27*(5), 890-898.

Lee, J. I., Scanlon, A., & Scanlon, M. A. (2007). Effect of early age loading on time-dependent deflection and shrinkage restraint cracking of slabs with low reinforcement ratios. *Special Publication, 246*, 149-166.

Nejadi, S. (2005). Time-dependent cracking and crack control in reinforced concrete structures. University of New South Wales.

Newhook J. (2001). Reinforcing concrete structures with fibre reinforced polymers. ISIS Canada: Design Manual No.3, The Canadian Network of Centres of excellence on intelligent sensing for innovative structures, Winnipeg, Manitoba, Canada.

Park, H. G., Hwang, H. J., Hong, G. H., & Kim, J. Y. (2012). Immediate and long-term deflections of reinforced concrete slabs affected by early-age loading and low temperature. *ACI Structural Journal, 109*(3), 413.

Park, H. G., Hwang, H. J., Kim, J. Y., Hong, G. H., Im, J. H., & Kim, Y. N. (2010). Creep and effective stiffness of early age concrete slabs. *Proceeding of the Fracture Mechanics of Concrete and Concrete Structures–Assessment, Durability, Monitoring and Retrofitting of Concrete Structure*, 751-754.

Rafi, M. M., Nadjai, A., Ali, F., & Talamona, D. (2008). Aspects of behaviour of CFRP reinforced concrete beams in bending. *Construction and Building Materials, 22*(3), 277-285.

Vakhshouri, B., & Nejadi, S. (2014). Limitations and uncertainties in the long-term deflection calculation of concrete structures. In Vulnerability, Uncertainty, and Risk: Quantification, Mitigation, and Management (pp. 535-546).

Vollum, R. L. (2003). Multipliers for deflections in reinforced concrete flat slabs.

Yost, J. R., Gross, S. P., & Dinehart, D. W. (2003). Effective moment of inertia for glass fiber-reinforced polymer-reinforced concrete beams. *Structural Journal, 100*(6), 732-739.